

Quasiparticle spectra from molecules to bulk

Vojtěch Vlček,^{1,*} Eran Rabani,^{2,3,†} and Daniel Neuhauser^{1,‡}

¹*Department of Chemistry and Biochemistry, University of California, Los Angeles California 90095, U.S.A.*

²*Department of Chemistry, University of California and Materials Science Division, Lawrence Berkeley National Laboratory, Berkeley, California 94720, USA*

³*The Raymond and Beverly Sackler Center for Computational Molecular and Materials Science, Tel Aviv University, Tel Aviv, Israel 69978*

(Dated: August 15, 2017)

A stochastic cumulant GW method is presented, allowing us to map the evolution of photoemission spectra, quasiparticle energies, lifetimes and emergence of collective excitations from molecules to bulk-like systems with up to thousands of valence electrons, including Si nanocrystals and nanoplatelet. The quasiparticle energies rise due to their coupling with collective shake-up (plasmon) excitations, and this coupling leads to significant spectral weight loss (up to 50% for the low energy states), shortening the lifetimes and shifting the spectral features to lower energy by as much as 0.6 eV. Such features are common to all the systems studied irrespective of their size and shape. For small and low dimensional systems the surface plasmon resonances affect the frequency of the collective excitation and position of the satellites.

Recent developments in Green’s function (GF) techniques have allowed for the description of charge excitations, i.e., quasiparticles (QPs) [1, 2], in the bulk, over a wide range of QP energies. Band-edge excitations are well-described by the so called G_0W_0 approximation [3–5], while at higher QP energies corrections are required to account for charge-density fluctuations and hole-plasmon coupling [5–8]. Photoemission experiments on solids reveal significant QP lifetime shortening and coupling to other collective excitations, manifested by satellite structures in the photoemission spectra [6, 9, 10]. The satellite structure and the QP lifetime shortening is often captured by the cumulant expansion (CE) ansatz to G_0W_0 [6–8, 10–14].

In confined systems, the QP spectrum near the band-edge is governed by the quantum confinement of electrons and holes. Higher energy, satellite-excitations are attributed to simultaneous ionization and excitation of the valence electrons (“shake-up” excitations) [13, 15–18]. Transition and differences between the satellite spectral features of molecules and nanostructures with “shake-up” signatures and bulk with collective plasmon resonances have been difficult to assess, as they require many-body treatment of systems with hundreds and thousands of electrons. In fact, the quantum confinement effect on the satellite transitions has received little attention if any.

In this letter, we address this challenge by combining the well-known cumulant expansion (CE) ansatz [5, 7–9, 11, 19, 20] with the recent stochastic GW approach (sGW [21, 22]), to obtain a nearly linear-scaling algorithm that reveals the changes of the QP spectra from a single molecule to covalently bonded nanocrystals (NCs) of unprecedented size (here up to 5288 valence electrons). The formalism is presented and assessed for the two size extremes (molecule and bulk), followed by the study of the effects of quantum confinement on the satellite structure in silicon NCs of different size and shape. In small

NCs the satellite features are affected by the changes in the plasmon energy. For large NCs, we find observable quantum confinement effects on the satellite features below the exciton Bohr radius, where the position of the satellite peak and the QP lifetime show small dependence on the size of the system.

The central theoretical quantity for quasiparticles is the spectral function, which in the sudden approximation is directly linked to the photoemission current [5, 23, 24]. The spectral function of the i^{th} QP state is $A_i(\omega) = \frac{1}{\pi} \text{Im}G_i(\omega)$, where the Green’s function fulfills the Dyson equation $G_i(\omega) = G_i^{(0)}(\omega) + G_i^{(0)}(\omega)\Sigma_i(\omega)G_i^{(0)}(\omega) + \dots$, where $G_i^{(0)}(\omega)$ is the non-interacting Green’s function and Σ_i is the self-energy. All the quantities are non-local in space and all the higher terms in the equation represent a convolution integral, but for brevity we omit the spatial dependence in the notation.

As usual, the non-interacting system is described by the Kohn-Sham DFT [25, 26] (see details in [27]). The self energy is then given in the diagonal G_0W_0 approximation as [3]: $\tilde{\Sigma}_i(t) = i \langle \phi_i | \tilde{G}_i^{(0)}(t) W(t^+) | \phi_i \rangle$, where t^+ is infinitesimally after t , ϕ_i is the KS eigenstate, $W(\omega) = \epsilon^{-1}(\omega)v_c$, v_c is the Coulomb kernel and $\epsilon^{-1}(\omega)$ is the inverse dielectric function. Quantities in frequency (G and Σ) and time domains (\tilde{G} and $\tilde{\Sigma}$) are simply related by their Fourier transforms. From the calculated $\Sigma_i(\omega)$ the G_0W_0 spectral function is given by:

$$A_i^{GW}(\omega) = \frac{1}{\pi} \frac{|\text{Im}\Sigma_i(\omega)|}{(\omega - \varepsilon_i - \text{Re}\Sigma_i(\omega) + \bar{v}_{XC})^2 + (\text{Im}\Sigma_i(\omega))^2}, \quad (1)$$

where ε_i is the KS eigenstate energy and \bar{v}_{XC} is the expectation value of the mean-field exchange-correlation potential. A_i^{GW} has peaks at the quasi-particle energies, ε_i^{qp} , that fulfill the fixed-point equation,

$$\varepsilon_i^{qp} = \varepsilon_i + \text{Re}\Sigma_i(\omega = \varepsilon_i^{qp}) - \bar{v}_{XC}. \quad (2)$$

In this GW approximation, the inverse lifetime of the QP is given by the imaginary part of the self-energy at the peak. However, the actual plasmon-hole coupled excitations are not in general represented by the isolated poles in Eq. (1) and $A^{GW}(\omega)$ thus does not yield a proper description of satellite structures. In addition, spurious secondary peaks arise if Eq. (2) has multiple solutions [6, 7, 20].

The CE formulation is required to account for the effect of hole-plasmon coupling. For the i^{th} occupied state, the Green's function in the CE *ansatz* reads [5, 9, 19]:

$$\tilde{G}_i(t) = -ie^{i\varepsilon_i t} e^{C_i(t)} \theta(-t) = -ie^{i\varepsilon_i t + C_i^{qp}(t)} e^{C_i^s(t)} \theta(-t), \quad (3)$$

where C_i is the cumulant, obtained from the Dyson series expansion. Further, following Ref. [6] the cumulant contribution is separated into two components. The first is a QP cumulant, C_i^{qp} , derived explicitly in Ref. [6] and associated with a portion of the spectral function describing the main QP peak:

$$A_i^{qp}(\omega) = \frac{\mathbf{Z}_i}{\pi} \frac{|\text{Im}\Sigma(\varepsilon_i^{qp})|}{(\omega - \varepsilon_i^{qp})^2 + (\text{Im}\Sigma(\varepsilon_i^{qp}))^2}, \quad (4)$$

where the renormalization factor, due to redistribution of the spectral weight into the satellite peaks, is $\mathbf{Z}_i = e^{\alpha_i}$ with $\alpha_i = \left. \frac{\partial \Sigma(\omega)}{\partial \omega} \right|_{\omega=\varepsilon_i}$. The lifetime of the QP is $1/|\text{Im}\Sigma(\varepsilon_i^{qp})|$.

By itself, $A_i^{qp}(\omega)$ does not include any satellite contributions – it is a single Lorentzian-shaped peak around the QP energy. The satellite peaks stem from resonances identified as poles in $W(\omega)$ (i.e., zeros of $\varepsilon(\omega)$) and appear as strong maxima in the imaginary part of the self-energy; they are introduced by the second part of the exponential in Eq. (3) that derives from the spectral representation of Σ_P [6, 9, 19]:

$$C_i^s(t) = \frac{1}{\pi} \lim_{\eta \rightarrow 0} \int_{-\infty}^{\mu} \frac{\text{Im}\Sigma_P(\omega) e^{-i(\omega - \varepsilon_i + i\eta)t}}{(\omega - \varepsilon_i + i\eta)^2} d\omega. \quad (5)$$

We solve for $C_i^s(t)$ using Σ_P , obtained from the stochastic G_0W_0 calculation. The computed satellite cumulant, $C_i^s(t)$, is inserted to Eq. (3) which is Fourier transformed to yield $G_i(\omega)$, and thereby $A_i(\omega) = \text{Im}(G_i(\omega))$ [28].

We next verify our approach using a large NC, $\text{Si}_{705}\text{H}_{300}$, that is close to the bulk limit. Fig. 1 shows the spectral function of the bottom valence band (VB - denoted A_b^{GW}) with a pronounced QP peak at -17.5 eV. If a cumulant expansion is not used, A_b^{GW} shows an additional maximum at -39.8 eV. This is in excellent agreement with previous GW calculations for bulk systems, but is not observed experimentally, and is attributed to spurious secondary solutions to Eq. (2) [6–8, 10, 11].

With the cumulant *GW* (Eq. (3)) the spectrum changes drastically and an additional peak is obtained

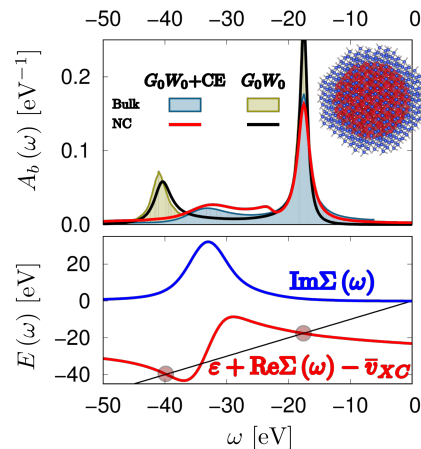


FIG. 1. **Top:** Spectral function for the bottom VB, $A_b(\omega)$, for a bulk solid from Ref. [10] and for $\text{Si}_{705}\text{H}_{300}$ NC. The G_0W_0 +cumulant spectral function (red) has an asymmetric satellite peak at the maximum of $\text{Im}\Sigma(\omega)$. The G_0W_0 prediction (black) has an artificial second maximum at low energies due to a spurious additional solution of Eq. (2). The inset plots the structure of the nanocrystal and orbital density isosurface (red; Si and H are blue and white circles). **Bottom:** Graphical solutions to the QP equation, marked with red circles, are found at the intersection of the red curve ($\varepsilon + \text{Re}\Sigma(\omega) - \bar{v}_{XC}$) with the diagonal ω line.

at -32.3 eV in excellent agreement with a result for bulk Si [10]. This peak is physically meaningful as it corresponds to the maximum of $\text{Im}\Sigma(\omega)$ associated with a collective excitation of the valence electrons (plasmon). The appearance of the satellite structure is accompanied by reduction of the intensity of the main QP peak, so that the renormalization factor is $\mathbf{Z} = 0.61$, i.e., 39% of the intensity is transferred to the satellites. The asymmetry of the satellite is due to the difference between the effective masses of the QP and the plasmon [12]. The pronounced transfer of the spectral weight to the plasmon satellite for the bottom valence excitations is a consequence of their high energy and spatial extent (leading to large overlaps with other states). An isosurface of the bottom valence orbital of $\text{Si}_{705}\text{H}_{300}$ indeed exhibits spherical symmetry and lacks nodal planes as seen from the inset of Fig. 1.

To further test our approach on finite systems, we applied (Fig. 2) the stochastic G_0W_0 approximation with CE to a series of small molecules for which experimental photoemission spectra are available. The results in Fig. 2 were further scaled so that the bottom valence state peak has the same intensity as the G_0W_0 +CE curve. The G_0W_0 +CE description relies on the concept of plasmon, valid for extended systems. It is thus surprising that this approach provides a qualitative description for such small systems. Indeed, the stochastic *GW* with damped real-time propagation of the excited state [21, 22] is in qualitative agreement with experiment and with high level SAC-CI (symmetry-adapted-cluster configuration inter-

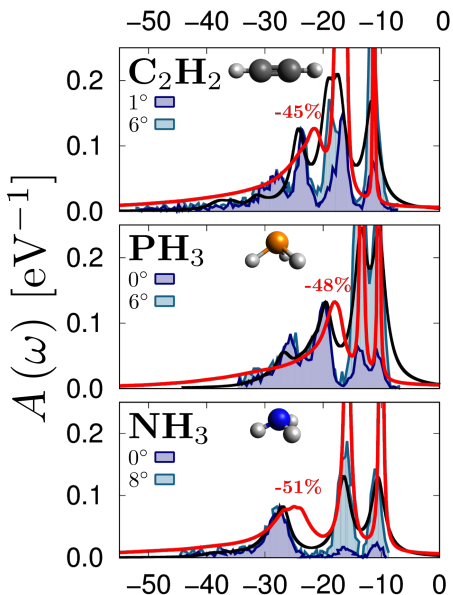


FIG. 2. Spectral functions (red line) from stochastic G_0W_0+CE for C_2H_2 , PH_3 and NH_3 . The spectral weight loss from the bottom valence state to the satellites is shown above the peak. Theoretical spectra obtained with SAC-CI [29, 30] are in black and the colored areas refer to the experimental photoemission spectra for two relative azimuthal angles [30, 31].

action) calculations, computationally feasible for small molecules [32]. We note that:

(i) the QP energies at the top valence band are captured well by G_0W_0 . This is the energy region where DFT is a good starting point. But G_0W_0 fails, however, to reproduce the bottom end of the valence band, where it underestimates the position of the peaks by a significant amount of 2 eV. For these states, DFT is not a good starting point and the “single-shot” G_0W_0 procedure is inaccurate.

(ii) Most importantly, the G_0W_0+CE description captures the satellite overall decay, although without the fine structure peaks in the satellite region. The pronounced satellite spectral weight comes at the expense of the QP peaks which transfer up to 51% of their intensity to the satellite tails. The broadening of the satellite peaks observed in G_0W_0+CE is a consequence of an intrinsic decay of the density–density correlation function in time (τ). The peak width is independent of the maximal time used to simulate the screening (we have varied the propagation time from 1 to 24 fs without affecting the lifetime), leading to a set of broad poles in the dielectric function. In theory, an infinite propagation time would result in sharp poles due to recurrences in the correlation function. As clearly can be seen in Fig.2, accounting only for τ yields a photoelectron spectrum in good agreement with experiment, likely due to other mechanism suppressing the recurrences in photoelectron spectroscopy.

Further, the G_0W_0+CE spectral function has maxima that are shifted with respect to the G_0W_0 QP energies. The shift is large for the bottom valence states; e.g., for NH_3 the G_0W_0 peak is at -25.0 eV while the G_0W_0+CE maximum is at -25.7 eV. The 0.7 eV difference is significant as it is 17% of the GW correction to the LDA energy (-20.8 eV). Thus, the usual practice where G_0W_0 results are directly compared to photoionization experiment is problematic, especially for low energy states, as it does not include the coupling of these states to the shake-up excitations.

In the next, main, part of this letter we investigate the evolution of the spectral function with system size; the results for a series of Si NCs (normalized by the number of electrons) are shown in Fig. 3. All NCs exhibit a discrete and narrow spectrum near the top of the VB. Due to the quantum confinement effect, the top of the VB shifts to higher energies with increasing size; the highest occupied state has energies of -8.1 eV and -6.4 eV for $Si_{35}H_{36}$ and for $Si_{1201}H_{484}$, respectively. For deeper hole excitations, the sharp features merge into a semi-continuous spectral response with significant life-time shortening. This is accompanied by significant spectral weight transfer ($\sim 50\%$) to the satellites. The bottom of the VB depends weakly on the system size, spanning an energy between -17.3 and -17.7 eV for the range of NCs studied. The QP peak also overlaps with the emerging satellite, which is already well-developed into its bulk shape for $Si_{35}H_{36}$ and found in the range typical for bulk silicon [7]. This result is rather surprising, since both the QP spectrum near the band edge and the plasmonic excitations are sensitive to the system size. We further observe that the dimensionality does not strongly affect the main QP peaks: the silicon platelet has $\sim 60\%$ of the Si atoms on the surface, yet its spectral function is similar to the NCs.

On closer inspection, we observe that the satellite maximum exhibits non-monotonic shifts: First it shows a strong decrease in energy for systems from $Si_{35}H_{36}$ to $Si_{705}H_{300}$ (from -22.5 to -26.1 eV, respectively), which is followed by slight move back to higher energies by 0.6 eV. The initial regime stems from the decrease in the plasmon resonance frequency (ω_p) discussed below in detail. Once ω_p converges, the satellite maximum follows the changes in the QP DOS of the valence states governed by quantum confinement, i.e. the spectrum moves to higher energies (c.f., Fig. 3).

In Fig. 4 we show $Im\Sigma_P(\omega)$ together with the graphical solution to Eq. 2 (which also depicts spurious secondary solutions found already for $Si_{35}H_{36}$ at -36 eV). The plasmon peak in the $Im\Sigma_P(\omega)$ curve changes till the asymptotic limit is reached; ultimately the curve for NCs with 3120 electrons ($Si_{705}H_{300}$) and 5288 electrons ($Si_{1201}H_{484}$) have practically identical height, width and position. The distance between the maximum of $Im\Sigma_P(\omega)$ and the QP energy corresponds to ω_p cou-

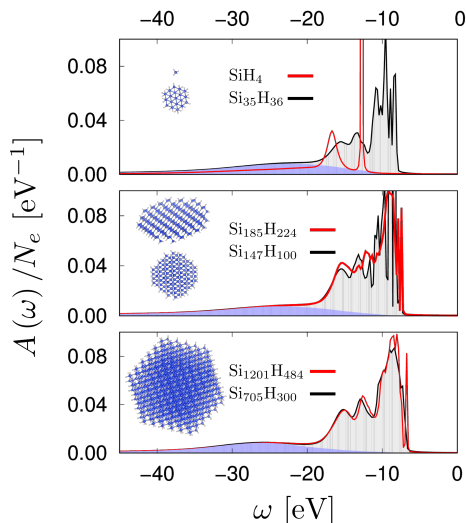


FIG. 3. Spectral functions for silicon nanocrystals, a platelet (middle panel - red) and a silane molecule. Satellite contributions to the spectral function are shown by a blue shaded area.

pled to the bottom valence hole; for the largest system $\omega_p = 15.3$ eV. Convergence of ω_p with system size is shown in the inset for the top and the bottom VBs.

Unlike in solids, the holes in finite systems couple to two types of plasmon resonances: low energy surface plasmon and high energy bulk plasmon. For small NCs, both contribute and lead to a broad peak in $\text{Im}\Sigma_P(\omega)$. The surface plasmon resonances also strongly contribute in low dimensional structures – the plasmon satellite of the large Si platelet has a maximum at -22.6 eV which is almost identical to the smallest NC ($\text{Si}_{35}\text{H}_{36}$). For big systems, the hole becomes more localized inside the NC (c.f., inset of Fig. 1) and the coupling to the bulk plasmon dominates, leading to increase in ω_p . The distribution of the resonances becomes more narrow and the peak in $\text{Im}\Sigma_P(\omega)$ decreases in width.

In summary, our calculations are the first ab-initio theoretical predictions of the photoemission spectra, quasi-particle energies and lifetimes covering the wide region between molecules and solids. The calculations show that the QP energies gradually increase with system size and this is accompanied by changes in the position of the satellite peaks which corresponds to a simultaneous ionization of the system and creation of a collective (shake-up or plasmon) excitation. The characteristic frequency of the plasmon has a narrower energy distribution in comparison to the shake-up but both are similar in nature and significantly alter the spectrum at low energies. Further, we have shown that for small systems the satellite region merges with the QP peak and shifts the apparent photoemission peak maximum to lower energies. The QP energies and photoemission maxima thus differ for the systems studied by as much as 0.6 eV.

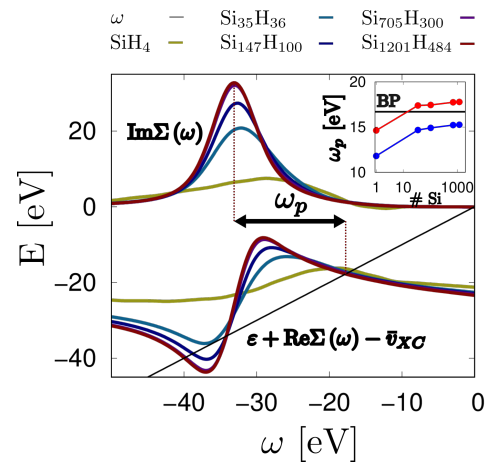


FIG. 4. Results for the bottom VB of Si nanocrystals of different sizes: Upper lines (above $E=0$) show the imaginary part of the self-energy. Lower curves below $E=0$ give the shifted real part of the self energy and represent the graphical solution to Eq. 2 (the QP energy is the intersection with the frequency line in black). The plasmon resonance (ω_p) for the bottom VB hole is shown in the inset for the bottom VB (blue) and for the top VB (red) together with the experimental value of the bulk and surface plasmon (BP - Ref. [33]) shown by a black vertical line.

The position of the satellite region is dictated by the QP energies and the frequency of the collective excitation. For small and low dimensional systems, surface and bulk plasmon resonances contribute to the satellites (leading to inhomogeneous broadening of the satellites). With increasing size the higher energy bulk plasmon coupling dominates. For small and intermediate systems, the maximum of the satellite decreases in energy and is affected by the plasmon resonance energy. For big systems, the maximum shows a slight increase due to changes in the main part of the QP spectrum.

This work was supported by the Center for Computational Study of Excited-State Phenomena in Energy Materials (C2SEP) at the Lawrence Berkeley National Laboratory, which is funded by the U.S. Department of Energy, Office of Science, Basic Energy Sciences, Materials Sciences and Engineering Division under Contract No. DE-AC02-05CH11231, as part of the Computational Materials Sciences Program. The calculations were performed as part of the XSEDE computational project TG-CHE160092 [34]. This research used resources of the National Energy Research Scientific Computing Center, a DOE Office of Science User Facility supported by the Office of Science of the U.S. Department of Energy under Contract No. DE-AC02-05CH11231.

* vojtech@chem.ucla.edu

† eran.rabani@berkeley.edu

‡ dxn@ucla.edu

- [1] Alexander L Fetter and John Dirk Walecka. *Quantum Theory of Many-Particle Systems*. Dover Publications, 2003.
- [2] E.K.U. Gross, E Runge, and O Heinonen. *Many-particle Theory*. A. Hilger, 1991.
- [3] Lars Hedin. New Method for Calculating the One-Particle Green's Function with Application to the Electron-Gas Problem. *Phys. Rev.*, 139(3A):A796—A823, aug 1965.
- [4] M S Hybertsen and S G Louie. Electron correlation in semiconductors and insulators: Band gaps and quasiparticle energies. *Phys. Rev. B*, 34:5390, 1986.
- [5] Richard M Martin, Lucia Reining, and David M Ceperley. *Interacting Electrons*. Cambridge University Press, 2016.
- [6] Ferdi Aryasetiawan, Lars Hedin, and Krister Karlsson. Multiple plasmon satellites in Na and Al spectral functions from ab initio cumulant expansion. *Phys. Rev. Lett.*, 77(11):2268, 1996.
- [7] Matteo Guzzo, Giovanna Lani, Francesco Sottile, Pina Romaniello, Matteo Gatti, Joshua J Kas, John J Rehr, Mathieu G Silly, Fausto Sirotti, and Lucia Reining. Valence electron photoemission spectrum of semiconductors: Ab initio description of multiple satellites. *Phys. Rev. Lett.*, 107(16):166401, 2011.
- [8] JJ Kas, John J Rehr, and Lucia Reining. Cumulant expansion of the retarded one-electron Green function. *Phys. Rev. B*, 90(8):085112, 2014.
- [9] David C Langreth. Singularities in the x-ray spectra of metals. *Phys. Rev. B*, 1(2):471, 1970.
- [10] Johannes Lischner, GK Pálsson, Derek Vigil-Fowler, S Nemsak, J Avila, MC Asensio, CS Fadley, and Steven G Louie. Satellite band structure in silicon caused by electron-plasmon coupling. *Phys. Rev. B*, 91(20):205113, 2015.
- [11] Fabio Caruso, Henry Lambert, and Feliciano Giustino. Band structures of plasmonic polarons. *Phys. Rev. Lett.*, 114(14):146404, 2015.
- [12] Derek Vigil-Fowler, Steven G Louie, and Johannes Lischner. Dispersion and line shape of plasmon satellites in one, two, and three dimensions. *Phys. Rev. B*, 93(23):235446, 2016.
- [13] James McClain, Johannes Lischner, Thomas Watson, Devin A Matthews, Enrico Ronca, Steven G Louie, Timothy C Berkelbach, and Garnet Kin-Lic Chan. Spectral functions of the uniform electron gas via coupled-cluster theory and comparison to the GW and related approximations. *Phys. Rev. B*, 93(23):235139, 2016.
- [14] Matthew Z Mayers, Mark S Hybertsen, and David R Reichman. Description of quasiparticle and satellite properties via cumulant expansions of the retarded one-particle Green's function. *Phys. Rev. B*, 94(8):081109, 2016.
- [15] J Schirmer, LS Cederbaum, and O Walter. New approach to the one-particle Green's function for finite Fermi systems. *Phys. Rev. A*, 28(3):1237, 1983.
- [16] LS Cederbaum, W Domcke, J Schirmer, and W Von Niessen. Correlation effects in the ionization of molecules: breakdown of the molecular orbital picture. *Adv. Chem. Phys.*, 65:115–159, 1986.
- [17] Michael S Deleuze and Lorenz S Cederbaum. Correlation effects in the valence x-ray photoionization spectra of ethylene, butadiene, and hexatriene. *Int. J. Quantum Chem.*, 63(2):465–481, 1997.
- [18] Anna I Krylov. The quantum chemistry of open-shell species. *Rev. Comput. Chem.*, 30, 2017.
- [19] BI Lundqvist. Single-particle spectrum of the degenerate electron gas. *Physik der kondensierten Materie*, 6(3):193–205, 1967.
- [20] Johannes Lischner, Derek Vigil-Fowler, and Steven G Louie. Physical origin of satellites in photoemission of doped graphene: An ab initio GW plus cumulant study. *Phys. Rev. Lett.*, 110(14):146801, 2013.
- [21] Daniel Neuhauser, Yi Gao, Christopher Arntsen, Cyrus Karshenas, Eran Rabani, and Roi Baer. Breaking the Theoretical Scaling Limit for Predicting Quasiparticle Energies: The Stochastic GW Approach. *Phys. Rev. Lett.*, 113(7):076402, aug 2014.
- [22] Vojtěch Vlček, Eran Rabani, Daniel Neuhauser, and Roi Baer. Stochastic GW calculations for molecules. *arXiv preprint arXiv:1612.08999*, 2016.
- [23] F Aryasetiawan and O Gunnarsson. The GW method. *Reports Prog. Phys.*, 61(3):237–312, mar 1998.
- [24] G Onida, L Reining, and A Rubio. Electronic excitations: Density-functional versus many-body Green's-function approaches. *Rev. Mod. Phys.*, 74:601, 2002.
- [25] P Hohenberg and W Kohn. Inhomogeneous electron gas. *Phys. Rev.*, 136:864, 1964.
- [26] W Kohn and L J Sham. Self-consistent equations including exchange and correlation effects. *Phys. Rev.*, 140:A1133, 1965.
- [27] The LDA DFT calculation used a real-space grid and Troullier-Martins pseudopotentials. The QP energies were calculated by the *sGW* approach detailed in [21, 22]. The grid spacings were $0.6a_0$ for the Si nanocrystals, $0.4a_0$ for the PH_3 and NH_3 molecules and $0.5a_0$ for the C_2H_2 molecule. The self-energy is approximated to be diagonal in the basis of KS eigenstates.
- [28] In principle, the total spectral function requires the calculation of $A_i(\omega)$ for all occupied states, but this is numerically prohibitive except for very small systems. However, since the quasiparticle energies and the spectral functions vary smoothly with frequency [Vlcek et al. 2017, ArXiv:1701.02023] for the extended system studied here, we compute the spectral function for several selected states and interpolate the result. The number of states is increased till the interpolation is converged to within 0.1 eV To evaluate the total spectral function of the large systems in Fig. 3, a single Lorentzian peak was used to describe the satellites. We found that a third order polynomial fit to the quasiparticle energies and the parameters of the Lorentzian peaks is sufficient to yield QP energies and satellite positions within 0.4 eV, i.e. way better than the resolution of the predicted spectral functions. For systems up to $\text{Si}_{705}\text{H}_{300}$, we found that calculations for 5 independent states provide converged results. For $\text{Si}_{1201}\text{H}_{484}$ 3 calculations were performed.
- [29] H Wasada and K Hirao. Computational studies of satellite peaks of the inner-valence ionization of C_2H_4 , C_2H_2 and H_2S using the SAC CI method. *Chem. Phys.*, 138(2-3):277–290, 1989.
- [30] Mayumi Ishida, Masahiro Ehara, and Hiroshi Nakatsuji. Outer-and inner-valence ionization spectra of NH_3 , PH_3 , and AsH_3 : symmetry-adapted cluster configuration interaction general-R study. *J. Chem. Phys.*, 116(5):1934–1943, 2002.
- [31] Erich Weigold, K Zhao, and W Von Niessen. Study of the valence electronic structure of ethyne by electron momen-

- tum spectroscopy and Green function methods. *J. Chem. Phys.*, 94(5):3468–3478, 1991.
- [32] Similar to Ref. [30], the SAC-CI results were convoluted with a Lorentzian peak with 2 eV broadening.
- [33] J Stiebling. Optische Eigenschaften des einkristallinen Siliziums aus Elektronenenergieverlustmessungen. *Z. Phys.*, 31(4):355–357, 1978.
- [34] John Towns, Timothy Cockerill, Maytal Dahan, Ian Foster, Kelly Gaither, Andrew Grimshaw, Victor Hazelwood, Scott Lathrop, Dave Lifka, and Gregory D Peterson. XSEDE: accelerating scientific discovery. *Comput. Sci. Eng.*, 16(5):62–74, 2014.